IMPACT DAMAGE MODELLING OF COMPOSITE AEROSPACE STRUCTURES SUBJECT TO BIRD-STRIKE

Javid Bayandor*, Alastair Johnson, Rodney S. Thomson***, Mathew Joosten***
The Sir Lawrence Wackett Aerospace Centre
School of Aerospace, Mechanical and Manufacturing Engineering
Royal Melbourne Institute of Technology
**** Institute of Structures and Design, German Aerospace Center**
*****Cooperative Research Centre for Advanced Composite Structures Ltd.**

Abstract

One of the key aerospace design and manufacturing criteria that needs to be effectively foreseen and withstood is medium velocity impact conditions enforced by foreign object impacts, mainly bird-strike events. Since experimental impact testing is very costly, efforts have been made to numerically model such events with sufficient accuracy to represent real case scenarios and, consequently, to significantly reduce the minimum number of tests required for product approval processes. So far, very few numerical methodologies have been developed to describe the intricacies of the fluid-solid interactions as seen in bird collisions onto advanced composite structures with either through-the-thickness fracture or delamination being accounted for. This study aims at integrating the capabilities offered by a fluid-structure analysis methodology, Smooth Particle Hydrodynamics, with a cohesive composite fracture and delamination model in order to enable the determination of intricate inter-laminar structural damage as occurred in advanced aerospace composite sub-assemblies and structures.

1 Introduction

There has been a significant increase in the use of composite materials over the recent decades, particularly in high performance aerospace applications. This can be attributed to the high specific strength, specific stiffness, fatigue performance and design flexibility that composite materials can offer. Initially, composite materials were restricted to non-aerospace applications, but further development has led to their wide-spread use in aeronautics as well as space missions. Composite materials are anisotropic in nature and exhibit little or no plastic deformation past their material yield point. As a result of this inability to elastically deform, they are subjected to several failure mechanisms under critical impact loading conditions. These include transverse matrix cracking, fibre failure, and delamination. They are particularly susceptible to impact damage, caused by foreign object impacts (FOI). This is due to the relatively poor mechanical properties of the advanced composites in the through-the-thickness direction.

The civil aviation regulations strictly require that the aerospace composite structures undergo verification procedures before any airworthiness certificate can be issued. Currently, the impact response of these structures, except for a very limited range of scenarios, can only be examined through experimental trial, which can be extremely uneconomical. Therefore, to reduce the number of tests required for the design and certification of such structures, and their associated costs, more reliable, fast and slow design tools and methodologies are required to be developed. This has been pursued by previous studies through experimenting with a variety of analysis approaches using discretised explicit finite element (FE) and/or quasi-static constitutive models, depending on the type of application,

analysis and accuracy required. The models were all aimed to reproduce some or all of the complex failure mechanisms of a composite structure which, for instance, in the case of bird-strike, are triggered by severe deformation and complex viscous interaction of the bird, in its solid, transitional and fluid states, with the structure. However, there still exists a large degree of inconsistency between different simulation models and experimental results. This is in addition to the shortcomings of the earlier release FE codes to couple the fluid-solid interactions (e.g. as occurred during bird-strike) with intricate failure response of the composite structures, particularly when incorporating matrix softening and delamination damage. Hence, as the processing capacities of the computers and analytical resources of the codes continue to improve, it remains imperative to further the development of an inclusive methodology capable of accurately predicting the response of such structures to "coupled multi-state" impact loading conditions.

Bird-strike is one of the most important FOI scenarios, often defined as a medium level energy impact. During a bird-strike, the projectile (bird) experiences a significant deformation, incorporating a phase change. Several numerical modelling approaches have been used to simulate this behaviour, including Lagrangian (LAG), Eulerian, Arbitrary Lagrangian-Eulerian (ALE) and Smooth Particle Hydrodynamics (SPH). However, each method still requires more rigorous investigation into its strengths and limitations. The suitability of each of these analysis methods will be discussed in the following sections of the paper.

Given the above, the aim of the present study has been to effectively couple the delamination feature of an explicit code, Pam-Crash, with its fluid-solid interactive algorithm to create a suitable FE methodology capable of analysing a variety of advanced primary composite structures under a wide range of soft impact loading conditions. The paper hence continues by detailing the numerical procedure introduced that can lead to accurate derivation of the main results which, in particular, include the size and extent of the delamination damage. Prediction of such values has been of principle interest to the aerospace design phase when determining the structural integrity of a critical primary composite stiffened component based on its impact response to a low to medium level energy collision.

2 Fluid / Solid Coupling Problems

For impact velocities in excess of 50 *m/s*, a bird-strike can be defined as a hydrodynamic impact. This is since the yield strength of the bird is exceeded during the collision due to generation of large deceleration forces [1], causing the bird to disintegrate and undergo a phase change into the fluid state. During the initial impact, regions of extremely high shock (Hugoniot) pressures are formed at the fluid-solid interface. These high pressure regions give rise to an extremely high pressure front (shock wave) moving through the projectile. The shock wave propagates, with the speed of sound, throughout the projectile in the direction opposite to its initial impact velocity vector. In the case of a bird-strike, the shock wave shatters the bird's internal structure. This will reduce the remainder of the projectile (yet to hit the target) to a bulk of fluid-like matter flowing onto the target, this time, however, with a steady-state pressure, which spreads the impact load over and well beyond the impact zone.

The Hugoniot pressure can be determined using the following expression [9]:

$$P_H = \rho_0 U_S U_0 \qquad (1)$$

where U_0 and U_S are the impact velocity and shock velocity, respectively, and ρ_0 the initial density.

After the initial impact, a state of steady flow is formed. The steady flow pressure at this stage can be approximated by the non-linear Bernoulli relationship, which assumes that the bird material is both inviscid and incompressible [9]:

$$P_{SS} = k\rho_0 U_0^{\,2} \qquad (2)$$

where k is approximately 0.5 for an incompressible fluid. However, complementary parametric studies have found that this value will approach 1.0 for a bird.

During a solid-fluid interaction, the projectile experiences a significant deformation, which needs to be captured by the numerical model for accurate prediction of the structural response. As a result of this extensive projectile deformation, hence the associated distortion of its comprising FE mesh, numerical instability may arise, which can highly adversely affect the accuracy of the solution or contribute to its divergence.

2.1 Mathematical Representation of the Bird

2.1.1 Eulerian and Lagrangian Approaches

The LAG method is a robust numerical approach involving basic meshing of the projectile (as shown in Fig. 1 where the arrow denotes the direction of impact). When modelling a soft-body impact, such as a bird-strike, the model will experience significant mesh distortion. This results in a decreased elemental time-step (hence an increased computational cost) and reduced accuracy of the simulation, which may lead to premature termination of the analysis (if the volume of any element becomes negative, due to element distortion).

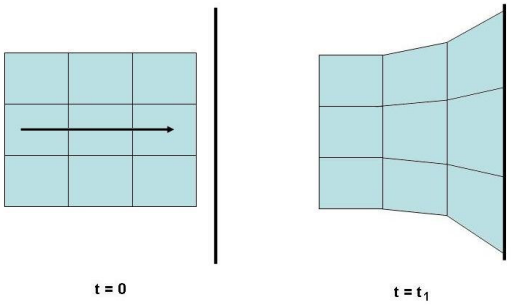

Fig. 1: Lagrangian mesh

In the Eulerian approach, a stationary mesh represents an extended control volume wrapped around the entire collision path of the projectile (Fig. 2). For soft impact events, the control volume considered needs to be wide enough to be able to enfold the highly deformed and diverging projectile during and after the impact. Although computationally intensive, this numerically stable approach is particularly suitable for modelling fluid-solid interaction, where, as indicated, the projectile undergoes a significant deformation. Nonetheless, the large number of elements required for the stationary mesh (encompassing the medium fluid, e.g. air in bird-strike events) and the associated high processing time are a disadvantage for practical application of this method to aerospace problems, as it often results in drastic increase of the computational cost of the analysis.

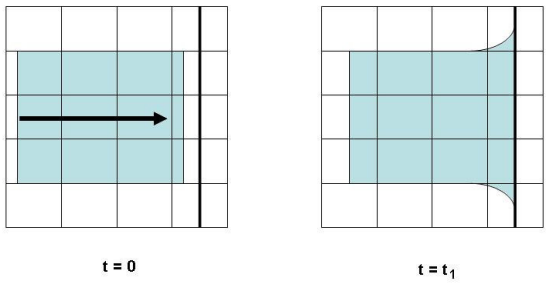

Fig. 2: Eulerian mesh

2.1.2 ALE Method

The ALE method attempts to address the significant shortfalls of both the LAG and the Eulerian methods by combining the efficiency of the LAG method with the stability of the Eulerian approach. An ALE simulation utilises a translating control volume with LAG mesh, coupled with an Eulerian projectile. In this approach, an expandable, yet much smaller, control volume of air surrounds the projectile only. The FE mesh, associated with the analysis space (LAG control volume), is a moving mesh that is capable of translating and expanding laterally while contracting longitudinally to follow the motion of the projectile during the impact. It creates an envelope around the deforming projectile which can contain the major part of the projectile mass (represented as a fluid after the initial impact). Since the ALE control volume is much smaller than the corresponding space in a pure Eulerian model, the computational time is significantly reduced.

ALE is inherently stable and can effectively adapt to large projectile deformations, hence, unlike LAG method, the ALE simulation will not be prematurely

terminated. This method has been successfully put to test by a number of authors [2],[3] for simulating bird-strike.

2.1.3 SPH Method

The SPH method is a meshless Lagrangian method which represents the projectile with a discrete set of interacting particles. In SPH, a user defined velocity field can be assigned to each of the particles that allows each particle to interact with the velocity fields of the neighboring particles through an approximate function. This approximate function has the same roll in SPH as that of the flexibility matrix in the Lagrangian method, relating each nodal displacement to the general displacement distribution throughout the entire structure.

The approximate function, also referred to as the 'kernel' or interpolation function, governs the SPH particles through the interpolation theory. The interpolation function defines the sphere of influence of each particle, hence the characteristics of the SPH element whilst in the vicinity of other elements. The sphere of influence in each particle is dependant on the smoothing length, h, of the particle, which can be either a fixed or variable parameter. The interpolation function is defined so that the particle does not exert any influence outside its sphere of influence. As the distance between particles approaches zero, the interpolation function must approach the delta function, the maximum inter-particular force, acting between two adjacent elements with overlapping smoothing lengths [4]. SPH models have proven to be stable for large deformations, and are significantly more efficient than Lagrangian, Eulerian or ALE simulations [5]. The accuracy of the solution is increased when the SPH particles are spaced as evenly as possible [5].

2.1.3.1 SPH modelling features of Pam

The SPH method has been incorporated into the Pam suite of analysis software, and has been used to simulate soft-body impact in a number of earlier studies [6],[4]. The geometry of a single SPH particle, as defined in Pam-Suite, is shown in Fig. 3. The figure depicts the assumed theoretical volume assigned to the particle (since the particle mass remains lumped at the centre of the SPH node) and the sphere of influence (which is twice the smoothing length, *h*).

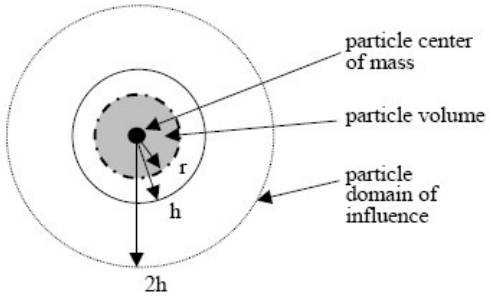

Fig. 3: SPH particle specifics [7]

Solid elements can be converted into SPH elements. This conversion process requires to create a node at the centroid of the solid element with an elemental volume assigned to this node. Subsequently, the original solid element has to be deleted, leaving a single node SPH element. With some manual interventions and user defined macros, this process can be adapted to transform a solid meshed entity to an equivalent model of SPH elements. Several interpolation functions are available within Pam-Crash which could then be associated to the SPH model generated to define its domain of influence over the neighbouring particles. These include W4 B-Spline, Q-Gaussian, Quartic and Quadratic. The SPH simulations presented in this paper have utilised the W4 B-spline interpolation function, shown in Fig. 4 below.

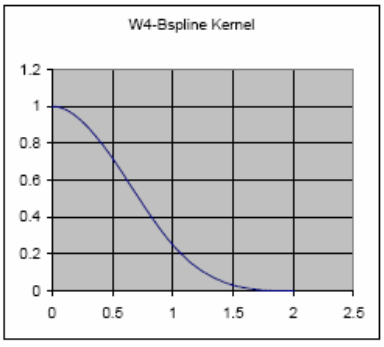

Fig. 4: W4 B-Spline interpolation function [7]

SPH particles can be subjected to loads or constraints as if they were nodes. FE-SPH coupling is achieved by the use of penalty contacts, where the SPH particles are defined as

the slave nodes. An SPH simulation example is illustrated in Fig. 5.

2.2 Composite Failure Modelling

During impact loading of composite structures failure may occur by delamination, which is important in lower energy impacts and in failure initiation, and by in-plane ply failure, which controls ultimate fracture and penetration in the structure. The composites failure models used through the Pam suite of explicit FE codes apply continuum damage mechanics (CDM) for composites as developed by Ladevèze [13] as a framework within which in-ply and delamination failure may be modelled. The mathematical failure models used and their FE implementations are as follows.

2.2.1 Elastic-plastic Fabric Composite Model

The fabric reinforced composite ply is modelled as a homogeneous orthotropic elastic or elastic-plastic damaging material whose properties are degraded on loading by micro-cracking prior to ultimate failure. A CDM formulation is often used to capture ply degradation parameters which are internal state variables governed by damage evolution equations [4]. For in-plane shear, deformations are controlled by matrix behaviour which may be inelastic, or irreversible, due to the presence of extensive matrix cracking or plasticity. On unloading, this can lead to permanent deformations in the ply. The extension of the fabric model to include these irreversible damage effects is now considered, based on the following additional assumptions:

a) The total strain in the ply is split into the sum of elastic and plastic (or inelastic) parts.
b) Plastic strains are associated only with the matrix dominated in-plane shear response.
c) A classical plasticity model is used with an elastic domain function and hardening law applied to the 'effective' stresses in the damaged material.
d) Inelastic or plastic strain increments are assumed to be normal to the elastic domain function.

Based on Ref. 4, the total strain ε can be written as the sum of elastic ε^e and plastic strains ε^p ($\varepsilon = \varepsilon^e + \varepsilon^p$). Here, a plane stress model for a thin ply is assumed and the fact that only the shear strains can contribute to plasticity ($\varepsilon_{11}^p = \varepsilon_{22}^p = 0$, $\varepsilon_{12}^p \neq 0$). Following [4], an elastic domain function can be introduced $F(\tilde{\sigma}_{12}, R)$ where $\tilde{\sigma}_{12}$ is the 'effective' shear stress $\tilde{\sigma}_{12} = \sigma_{12}/(1-d_{12})$ and R is an isotropic hardening function. $R(p)$ is a function of an inelastic strain variable p. The elastic domain function takes a simple form, since, as assumed, only the effective shear stress can lead to plastic deformation:

$$F = |\sigma_{12}|/(1-d_{12}) - R(p) - R_o \qquad (3)$$

where $R(0) = 0$ and R_o is the initial threshold value for inelastic strain behaviour.

The condition $F < 0$ corresponds to a stress state inside the elastic domain, where the material may be elastic damaging. It follows from the normality requirement (d) that $F = 0$, $\dot{F} = 0$, hence, from Eq. (3) it can be drawn that the plastic strain p is defined by:

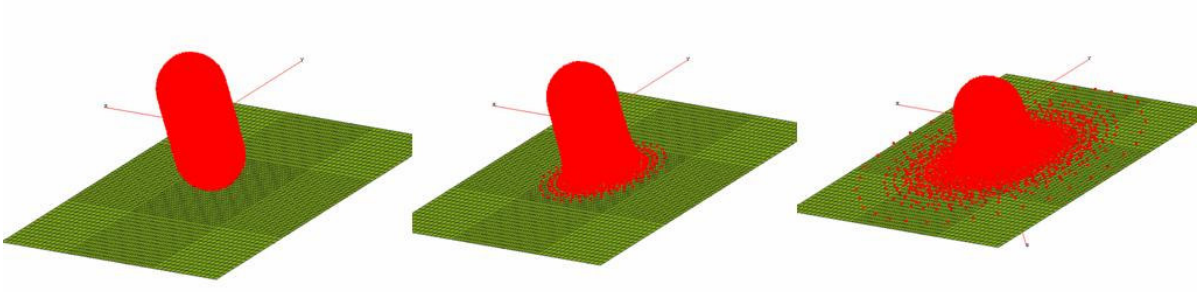

Fig. 5: An SPH impact simulation

$$\dot{\varepsilon}_{12}^{p} = \dot{p}/(1\text{-}d_{12})$$

or
$$p = \int_0^{\varepsilon_{12}^{p}} (1-d_{12})\, d\varepsilon_{12}^{p} \qquad (4)$$

where p is the accumulated effective plastic strain over the complete loading cycle. The model is completed by specifying the hardening function $R(p)$. This is determined from cyclic loading tests in which both the elastic and irreversible plastic strains are measured. A typical form assumed for the hardening function [4], which models test data fairly well, is an index function, which leads to the general equation:

$$R(p) = \beta p^{m} \qquad (5)$$

The shear plasticity model depends on the parameters β, the power index m and the yield stress R_o.

2.2.2 Damage and Delamination Models

Delamination damage, although not externally visible, contributes significantly to reducing the stiffness of the composite structure, which can ultimately lead to its premature failure under axial loading.

Delamination failures occur in composite structures under impact loads due to local contact forces in critical regions of the loading zone and at free edges. They are caused by the low, resin dominated, through-thickness shear and tensile properties found in laminated structures. In composites delamination models, the thin solid interface is modelled as a sheet of zero thickness, across which there is continuity of surface tractions but jumps in displacements [4]. The equations of the model are given here for the case of Mode I (peeling) tensile failure at an interface.

Let σ_{33} be the tensile stress applied at the interface, u_3 the displacement across the interface and k_3 the tensile stiffness. An elastic damaging interface traction-displacement model can then be defined as follows:

$$\left.\begin{aligned} \sigma_{33} &= k_3\,(1\text{-}\,d_3)\,u_3 \\ d_3 &= c_1\,(1 - u_{30}/u_3) \end{aligned}\right\} \qquad (6)$$

for $u_{30} \le u_3 \le u_{3m;}$ with tensile damage parameter d_3, and $c_1 = u_{3m}/(u_{3m} - u_{30})$. It can be verified that with this particular choice of damage function d_3, the traction-displacement function has the bi-linear or triangular form [4],[14]. u_{30} and u_{3m} correspond to the displacement at the peak stress $\sigma_{33m,}$ where the ultimate failure occurs. The damage evolution constants are defined in terms of σ_{33m} and G_{IC}, the critical fracture energy under Mode I interface fracture, by $u_{30} = \sigma_{33m} / k_3$ and $u_{3m} = 2G_{IC} / \sigma_{33m}$. They underline that the area under the traction-displacement curve is, in fact, equal to the fracture energy G_{IC}. Therefore, this interface model effectively represents an initially elastic interface, which is progressively degraded after reaching the maximum tensile failure stress of σ_{33m}, where the Mode I fracture energy can be fully absorbed as the failure is initiated and progressed. For Mode I inter-ply failure, the interface energy G_I, defined as

$$G_I = \int_0^{u_3} \sigma_{33}\, du_3 \qquad (7)$$

is monitored and, if found to exceed the critical fracture energy value G_{IC}, then the crack is allowed to advance.

For Mode II (shearing) interface shear fracture, a damage interface law similar to Eqs (6) is assumed, with equivalent set of damage constants u_{130} and u_{13m} and critical fracture energy G_{IIC}. In general, some form of mixed mode delamination failure, involving both shear and tensile failure, will also be present. This is incorporated in the model by assuming a Mixed Mode failure condition, which for Mode I-Mode II coupling can be represented by an interface failure envelope [4]:

$$\left(\frac{G_I}{G_{IC}}\right)^{n} + \left(\frac{G_{II}}{G_{IIC}}\right)^{n} = e_D \le 1 \qquad (8)$$

where G_I and G_{II} are the monitored interface strain energies in Modes 1 and 2, respectively, and G_{IC} and G_{IIC} are the corresponding critical fracture energies. The constant n is selected so that to fit the Mixed Mode fracture test data. Typically, n is found to be between 1 and 2.

Failure at the interface is imposed by degrading stresses when $e_D < 1$, using Eq. (6), and the corresponding shear relation. When $e_D \geq 1$, delamination occurs and the interface separates.

The explicit finite element (FE) software Pam-Crash was one of the explicit codes to have incorporated the above criteria. Using the composite failure features of this code, the delamination damage was determined through creating cohesive tied elements (non-linear spring, decohesion elements) between two (or more) layers of shell elements; the inter-laminar areas representing the anisotropic regions within a stack of composite plies.

The decohesion elements were connected together in the linear elastic range and modelled across the interfaces of the plies where the delamination was presumed to be initiated and propagated. This allowed the continuity of surface tractions within the FE model while enabling large displacements between the elements of the adjacent plies. A high initial stiffness was assumed to hold the top and bottom surfaces of the splitting structural plies together. After the normal and shear tractions for the decohesion elements reached their respective inter-laminar tensile or shear strengths, the stiffness was gradually reduced to zero. When the cohesive zone was no longer able to withstand any further impact load, the stiffness became zero and the delamination tip initiated or propagated further through the interface along the path of the earlier failed decohesion elements. The failure of the tied elements was dependent on the user defined variables, that include shear strength, Modes I and II fracture energies and the stresses required to both initiate and extend the delamination damage. Separate sensitivity analyses, outside the focus of this paper, were carried out to calibrate the delamination features of the code.

3 Explicit FE Simulation Approach

3.1 Representative Bird

Traditionally, bird strike tests have been conducted with real bird specimens. These tests have a large degree of scatter due to the complex and non-homogeneous composition of the birds [8]. In order to standardise the experiments however, 'representative' test birds have been introduced with cylindrical geometries and hemispherical end caps (HSE). The material used in such experimental testing is generally porous gelatine.

As for the simulation bird model, numerical studies have been carried out by a number of researchers including Wilbeck [9], who measured numerous birds of different size and weight, and concluded that the bird mass can be represented by a water air/mixture, with water making up to approximately 85-90% of the bird volume. This model was refined by Iannucci [10], who investigated two numerical bird models with different densities. The first model utilised a water/air mixture of 90% and 10%, respectively, where the second model consisted of 10% air, 85% water and 5% bone structure, which had slightly less compressibility than the pure water/air model. Several authors have adopted a similar approach to determine the density of a homogenous bird material, with the average density falling between 942-950 kg/m^3. The density of the material determines the dimensions of the bird model. The representative bird model, used in this study, is shown in Fig. 6, which has a length to diameter ratio (L/D) of 2.0.

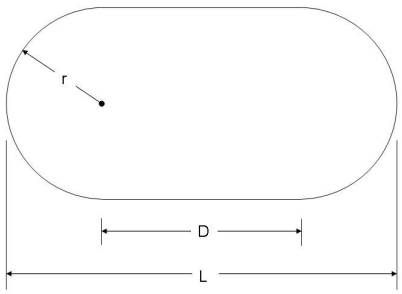

Fig. 6: Representative bird model

3.2 Meshing Approach

Since SPH is a meshless method, to create a series of SPH elements, conventional meshing procedures have to be modified. For the present work, it was necessary to have the SPH elements spaced as evenly as possible so as to increase the accuracy of the simulation. Unevenly spaced elements resulted in the adjoining particles 'pushing' against each other prior to the projectile impacting the target. This could cause the projectiles to start breaking up before the collision, hence instigating a large numerical error into the simulation results. In order to avoid this, a sequential cylindrical meshing scheme was introduced, which enabled an even element spacing through the thickness and along the length of the bird model. This approach further prevented the common SPH problem concerning the removal of the nodes shared between adjacent elements. The developed SPH particles (for the mid cross sectional station of the bird model) are shown in Fig. 7 [11].

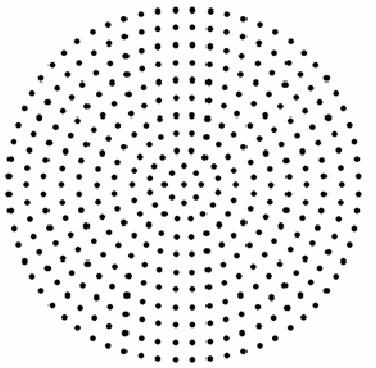

Fig. 7: Frontal view of SPH elements used in bird model

3.3 Material Modelling

Two of the material models available through Pam-preprocessor, Generis, are capable of simulating hydrodynamic behaviour of the bird. They are an 'Elastic-Plastic Hydrodynamic Solid' and the 'Murnaghan Equation of State (EOS)'. Several material constants are described for both material models. Since these constants cannot be directly measured, calibrating the model against experimental data was conducted (refer to [4]).

3.3.1 Elastic-Plastic Hydrodynamic Solid

For this material, the pressure-volume relationship is governed by an EOS, giving it the characteristics of an elastic-plastic material at low pressure. For a bird-strike the hydrodynamic behaviour of the numerical model is critical and determines how the bird can deform and transfer the loads onto the structure. The EOS for this material is represented by [7]:

$$P = C_0 + C_1\mu + C_2\mu^2 + C_3\mu^3 \qquad (9)$$

where C_is are material coefficients and μ is a dimensionless parameter, relating the material current density, ρ, to the initial density, ρ_0:

$$\mu = \frac{\rho}{\rho_0} - 1 \qquad (10)$$

3.3.2 Murnaghan EOS

Similar to the elastic-plastic hydrodynamic solid, the Murnaghan EOS is based on a state equation, prescribing a pressure-volume relationship for the material. The EOS is described by the following expression [7]:

$$P = P_o + B\left(\left(\frac{\rho}{\rho_o}\right)^{\gamma} - 1\right) \qquad (11)$$

where P_0 is a reference pressure and B and γ are material constants which describe the behaviour of the projectile. This material model was developed for solid and SPH elements, and has several advantages over the elastic-plastic hydrodynamic solid, including an increased time step and reduced pressure oscillations, compared to the elastic-plastic hydrodynamic solid. In addition, the material model does not require the definition of the material shear strength. Given the advantages of this material, the Murnaghan model was used for the numerical bird.

3.4 Initial Model Calibration

In this study, the material constants were determined by calibrating the pressure-time histories against experimental bird-strike data obtained from Wilbeck [9]. Wilbeck conducted

bird-strike experiments against a rigid steel plate, fitted with several pressure transducers, and measured the impact pressures at a number of locations. Of those pressures, the Hugoniot pressure, measured on impact, and the steady pressure, recorded after the initial strike against the target, were of principle importance and were used to calibrate the cylindrical SPH model.

For an SPH simulation, the pressure-time history cannot be directly obtained (since the impact zone is ever-changing). Therefore, the approach used to determine the instantaneous pressure was to convert the impact force to impact pressure through dividing it by the area of the progressive impact zone. At the moment of impact however, the contact area of the bird model was used, instead of the impact zone on the target, as a conversion parameter. This was since the impacted area of the target was infinitesimally small. However, since the SPH elements similarly did not have a sizable elemental area, the approximated contact area on the projectile was also minute, leading to an excessively large pressure history. As a result, it was decided to attempt to use the complete frontal area of the cylindrical bird (comprising of the entire area surrounded by the largest periphery of already collided SPH elements) to derive the Hugoniot pressure. This significantly reduced the percentage of error, however, was not able to fully eradicate it and leaving the results largely the overestimation of the theoretical value with the divergence of 43%.
In order to bring this inconsistency under control, a solid projectile, as also recommended by McCarthy et al. [6], was considered. This was since the pressure field for solid elements can be readily obtained during post-processing, hence providing a more accurate initial impact zone.

The pressure contours for an impact velocity of 180 *m/s* are shown in Fig. 8. The new calculated Hugoniot pressure, derived based on the initial impact area of the equivalent solid model, was only approximately 3% larger than the theoretical value.

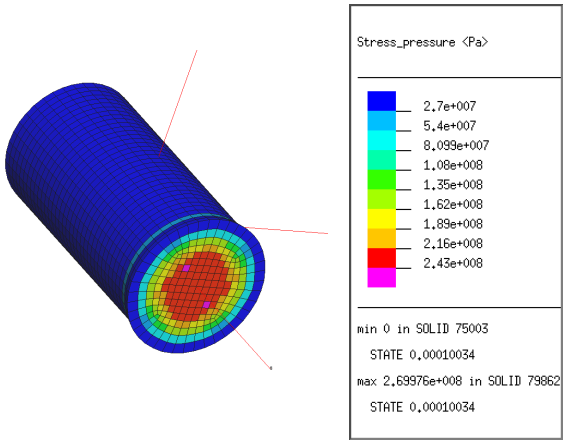

Fig. 8: Pressure contours of solid projectile

4 Simulation Modelling and Validations

In the modelling phase, initial calibrations for the SPH bird and delamination parameters were carried out using a rigid steel structure as a target and a SACME type composite fabric specimen with clamped boundary conditions, respectively.

Subsequently, an SPH bird was created and coupled with a composite leading edge structure, with active inter-laminar decohesion elements embedded within the structure. Decohesion elements (node-segment contacts) were applied between the wing structure (master) and the SPH nodes (slave). The initial impact velocity applied to the SPH nodes was perpendicular to the normal of the leading edge surface. The ply damage and delamination areas resulted from this soft impact are depicted in Fig. 9.

To validate the predicted structural damage for this idealised composite leading edge model, a comparison with available impact test data was required. The accuracy of the gas gun, used to obtain the said set of data, had already been established through an earlier work [4] by quantitative comparisons of the measured impactor force pulses from the drop weight tests and the acquisitioned strain gauge data from the gas gun tests to the corresponding variables obtained through representative FE simulations.

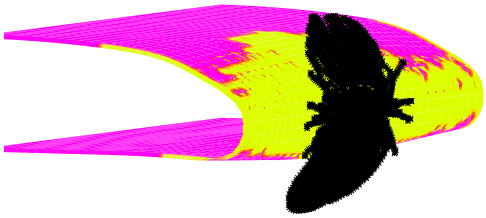

a) Delamination contours at 0.4 *ms*

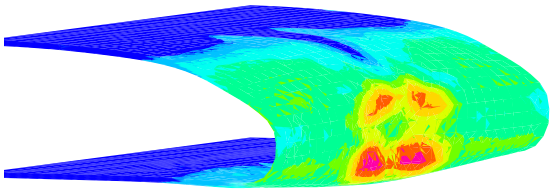

b) Ply damage contours at 0.4 *ms*

Fig. 9: Impact simulation of the glass fabric epoxy leading edge (M = 0.033 *kg*, V_0 = 200 *m/s*)

Attention was given to validation of the SPH soft body impactor model coupled with active composites shell damage and explicit delamination feature. The soft-body was simulated using gelatine projectile, correspondent to the properties of that used in the gas gun test. However, the validations were restricted to comparison of predicted total damage and delamination only, as detailed quantitative test data could not be obtained. This was since the gelatine projectile can easily disintegrate on impact and cannot be instrumented by an accelerometer. Also, the damage sustained, as a result of gelatine impact, by the strain gauges that were bonded onto the outer shell surface of the leading edge, limited the number of accurate strain field readings.

The impact tests were carried out at the Structural Integrity Department of the German Aerospace Center (DLR), Institute of Structures and Design. The composite leading edge shells were fabricated in glass fabric epoxy with a quasi-isotropic lay-up of $[0/45]_{2S}$ and nominal thickness of 2 *mm*. The shells had the length of 200 *mm*, with a sharp nose profile with the radius of 15 *mm*. For the tests, the shells were bonded onto a set of grooves on a steel-back plate, simulating a clamped edge boundary (BC) condition, with the curved edges left free. The cylindrical gelatine projectiles made had the diameter of 30 *mm* and the length of 40 *mm* with their masses in the range 30-34 *g*. The gelatine used was bovine hide gelatine (260 bloom). After the fabrication, the specimens ended up with a soft rubbery finish with coarse internal granular texture, which could be fragmented into smaller granules on impact.

The structure was impacted at the centre of the leading edge on the convex face at different impact velocities, chosen to give different levels of impact damage. Impact angles were parallel to the normal vector field of the structure. After the impacts, C-scan tests were carried out on the structure with a hand held probe to determine the extent of delamination damage, followed by marking of the delamination boundary on the structure. Three leading edge shells were tested at impact velocities of 132.5, 142.0 and 198 *m/s* selected to give a range of damage conditions. In all the tests, the gelatine cylinders disintegrated, flowing over the shell nose, as confirmed also by a series of high speed camera shots. This demonstrated that the impact loading imposed by gelatine was often spread over a wide area with little or no penetration into the target, a completely distinctive behaviour to that of the hard impactor. At the lowest impact velocity of 132.5 *m/s*, surface abrasion was observed, but no measurable delamination could be found through C-scanning. At 142.0 *m/s*, damage was initiated at the leading edge within the impact region. An increase of the impact velocity to 198 *m/s* resulted in formation of extensive delamination area over a much wider region as well as significant fibre cracking, as shown on the impacted specimen depicted in Fig. 10. In addition, an extensive cracking at the middle region of the curved shell wall was also detected which was well away from the point of impact. This had further prompted a considerable bending deformation of the structure, extended well beyond the nose region.

The matching simulations were set up and executed for impact velocities starting from 130 *m/s*. The lower impacts mainly led to elastic deformation in the shell, which returned to its original condition as the load was removed. Simulated impacts in the vicinity of 130 *m/s* caused some scattered and insignificant

delamination or fibre breakage. Computed results for normal impact at the centre of the leading edge at 200 *m/s*, as shown in Fig. 9, revealed that the SPH model had enough energy after the impact to flow over the leading edge in an almost identical manner to that observed during the tests. The fluid like surge of the impactor resulted in the spread of the collision load beyond the impact zone, where the inter-laminar fracture and delamination continued to be successfully captured by the decohesion elements embedded in the composite target.

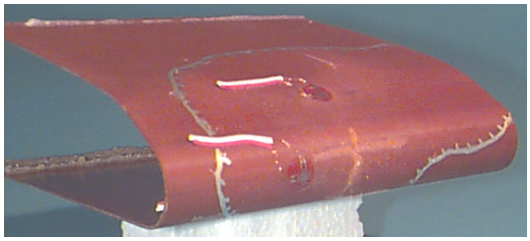

Fig. 10: Delamination area on impacted leading edge shell

Figure 9a shows the shell deformation at 0.4 *ms*, with highly deformed gelatine projectile and delamination damage, where Fig. 9b illustrates the middle ply damage contours at the same instance. Compared to the experimental results for the same velocity (Fig. 10), it is evident that the predicted delamination size is equivalent to that of the test. As mentioned, inclusive and detailed impact data, due to experimental constraints, could not be obtained. However, from the qualitative point of view, a good agreement between the simulation results and the tests, particularly for those pertaining to deformation and damage profiles, was acquired.

The methodology prescribed, incorporating a soft SPH impact coupled with stacked shell structural model, is deemed to be a promising predictive approach.

5 Conclusion

A predictive methodology has been introduced aiming at describing the intricacies of the fluid-structure interactions and failure mechanisms as seen in bird-strike events involving composite targets. Earlier studies have mostly focused on assessing the resulting impact damage sustained by metallic structures, or composite structures without inter-laminar fracture and delamination damage, etc. The present work investigated the feasibility of integrating the numerical simulation of highly deformable soft body impacts, through SPH modeling where the numerical mesh is replaced by interacting particles, with fibre reinforced composite primary structures damage and delamination analysis features.

For velocities ranging between 100 to 200 *m/s*, SPH impact simulations, combined with composites failure models (which incorporated ply damage and inter-ply delamination model), were carried out and compared with gelatine impact test data on glass fabric/epoxy cylinders. Encouraging results were obtained, indicative of the potential that the new methodology has to offer in assisting with the dynamic analyses involved during aerospace design and certification stages. Future work will consider the effect of composite materials rate dependency, refining the bird-strike predictive methodology and derivation of models suitable for simulation of advanced aerospace composite primary stiffened structures under a variety of foreign object impact conditions including burst tyres, hail stones and concrete and runway debris.

References

[1] Wilbeck JS and Barber JP. Bird impact loading. *The Shock and Vibration Bulletin*, Vol. 48, Part 2, pp 115-122, 1986.

[2] Langrand B, Bayart AS, Chauveau Y and Deletombe E. Assessment of multi-physics methods for bird strike modelling to a metallic riveted airframe. *Journal of Crashworthiness*, Vol. 7, pp 415-428, 2002.

[3] Hanssen AG, Girard Y, Olovsson L, Berstad T and Langseth M. A numerical model for bird strike of aluminium foam-based sandwich panels. *Journal of Impact Engineering*, Vol. 32, pp 1127-1144, 2006.

[4] Johnson AF and Holzapfel M. Modelling soft body impact on composite structures. *Composite Structures*, Vol. 61, pp 103-113, 2003.

[5] Anghileri M, Castelletti LML, Invernizzi F and Mascheroni M. A survey of numerical models for hail impact analysis using explicit finite element

codes, *Journal of Impact Engineering*, Vol. 31, pp 929-944, 2005.

[6] McCarthy MA, Xiao JR, McCarthy CT, Kamoulakos A, Ramos J, Gallard JP and Melito V. Modelling of bird strike on an aircraft wing leading edge made from fibre metal laminates – Part2: Modelling of impact with SPH bird. *Applied Composite Materials*, Vol. 11, pp 317-340, 2004.

[7] *ESI Pam-Crash solver notes*. Engineering Systems International, 2004.

[8] Budgey R. *The development of a substitute artificial bird by the International Birdstrike Research Group for use in aircraft component testing*. International Birdstrike Committee, IBSC25/WP-IE3, 2000.

[9] Wilbeck JS. *Impact behaviour of low strength projectiles*. Air Force Materials Laboratory, Technical report AFML-TR-77-134, 1977.

[10] Iannucci L. *Bird-strike impact modelling, foreign object impact and energy absorbing structures*. Institute of Mechanical Engineers, London, 1998.

[11] Joosten M. *Analytical and numerical investigation of advanced aerospace structures under impact loading conditions*. Aerospace Engineering Thesis, Royal Melbourne Institute of Technology, Melbourne, 2006.

[12] Bayandor J, Thomson RS, Scott ML, Nguyen MQ, Elder DJ. Investigation of impact and damage tolerance in advanced aerospace composite structures. *Journal of Crashworthiness*, Vol. 8, No. 3, pp 297 – 306, 2003.

[13] Ladevèze P. Inelastic strains and damage; Chapt. 4 in Damage mechanics of composite materials. *Composite Materials Series 9*, Elsevier, Amsterdam, 1994.

[14] Bayandor J, Thomson RS and Callus PJ. Impact performance substantiation of a novel replacement aerospace composite primary structure. *Proc. 11th Australian International Aerospace Congress,* Melbourne, The Royal Aeronautical Society and The Engineers, Australia, 2005.

Acknowledgements

The authors wish to acknowledge the contribution made by the other members of The Sir Lawrence Wackett Aerospace Centre Bird-strike Research Team to this work: Messrs D. Parekh, T. Purcell, D. Tata and T. Thi. Also, the contribution of Mr D. Elder from the Cooperative Research Centre for Advanced Composite Structures (CRC-ACS) is greatly acknowledged.

The respective funding and technical support offered by the Victorian Partnership for Advanced Computing, and Pacific-ESI, Australia, and ESI, France, has been instrumental for this project and is acknowledged. Special thanks go to Dr A. Pickett, Cranfield University, for implementation of the composites models in Pam-Crash while at ESI and his technical help.

The test programme and part of the simulation work were undertaken at the Structural Integrity Department of the German Aerospace Center (DLR), Institute of Structures and Design. The authors wish to express their gratitude for the assistance they have received from the DLR colleagues involved.